Statistical Monitoring and Early Forecasting of the Earthquake Sequence:

Case Studies after the 2019 M 6.4 Searles Valley Earthquake, California

Y. Ogata (Inst. Stats. Math., Tokyo) and T. Omi (Stockmark Inc., Tokyo)

Introduction

In the absence of any information, the probability of a major earthquake is very small. However, when information on "abnormal events" is available, the conditional probability increases to a greater or lesser extent. If you gather that information and apply the "multi-factor prediction equation", the probability of the forecast becomes practical (see Ogata, 2017a,b). Therefore, we need to take every opportunity to build up a series of short-term forecasting trials. As a notable recent example, we thought of the activity in the Ridgecrest, California area this time last year.

$$P(M\mid A,B,C)=\frac{1}{1+\left(\frac{1}{P_A}-1\right)\left(\frac{1}{P_B}-1\right)\left(\frac{1}{P_C}-1\right)\Big/\left(\frac{1}{P_0}-1\right)^{3-1}}\approx P_0\frac{P_A}{P_0}\frac{P_B}{P_0}\frac{P_C}{P_0}$$

$$\textbf{Probability gain}=\frac{\text{Conditional probability}}{\text{Baseline probability}}=\frac{\Pr(\text{Precursor of an large earthquake}\mid\text{Anomaly})}{\Pr(\text{Large earthquake})}$$

Aki (1981)

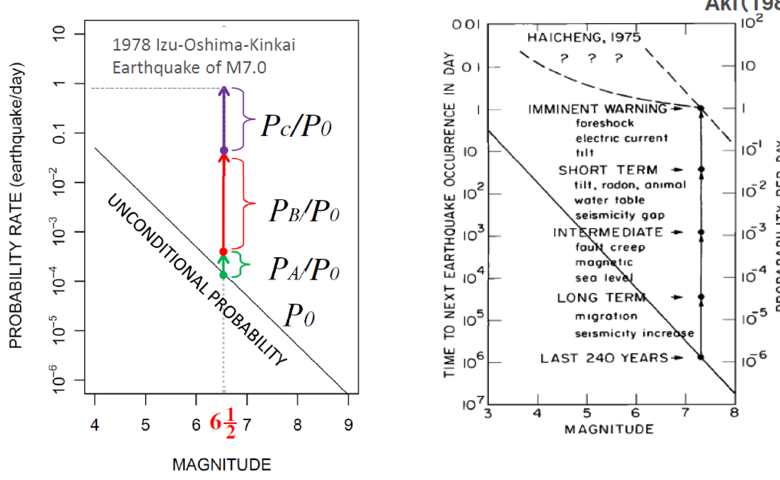

Space-time seismic activity monitoring

Delaunay tessellation of the Californian earthquakes. Delaunay triangles where the triangle vertices are the location of earthquakes of M ≥ 3 during the period 1932 - 2011, except for those on the boundaries of the rectangles.

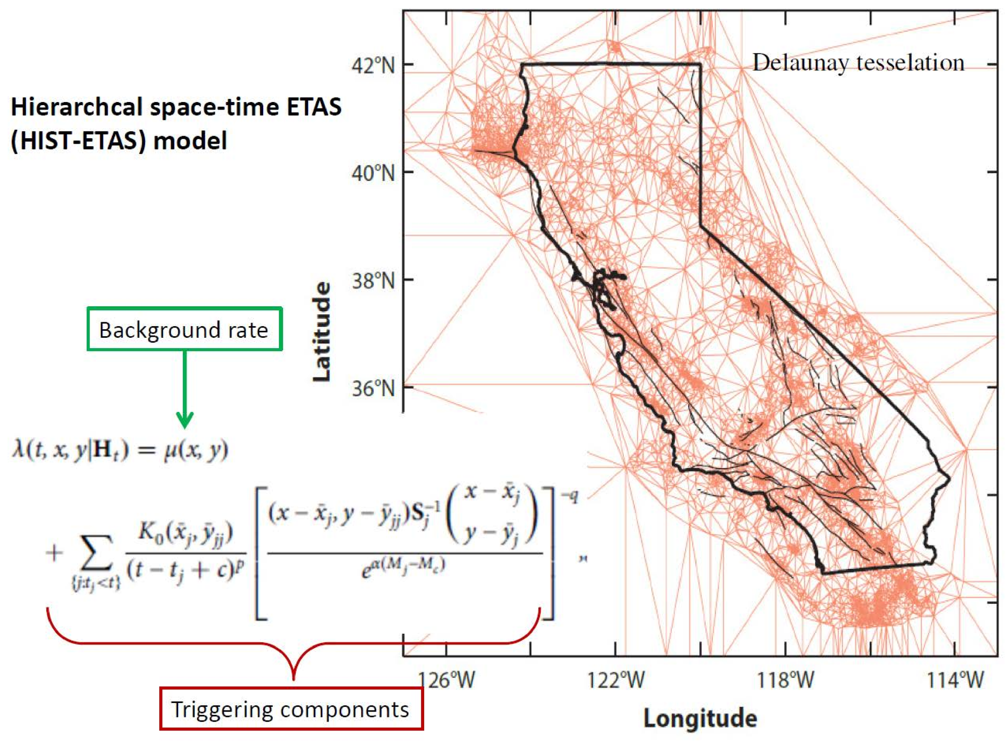

$$\lambda(t,x,y\mid H_t)=\mu(x,y)+\sum_{\{t_j<t\}}\frac{K_0(\bar{x}_j,\bar{y}_j)}{(t-t_j+c)^p}\left[\frac{(x-\bar{x}_j,y-\bar{y}_j)S_j^{-1}\binom{x-\bar{x}_j}{y-\bar{y}_j}}{e^{\alpha(M_j-M_c)}}\right]^{-q}$$

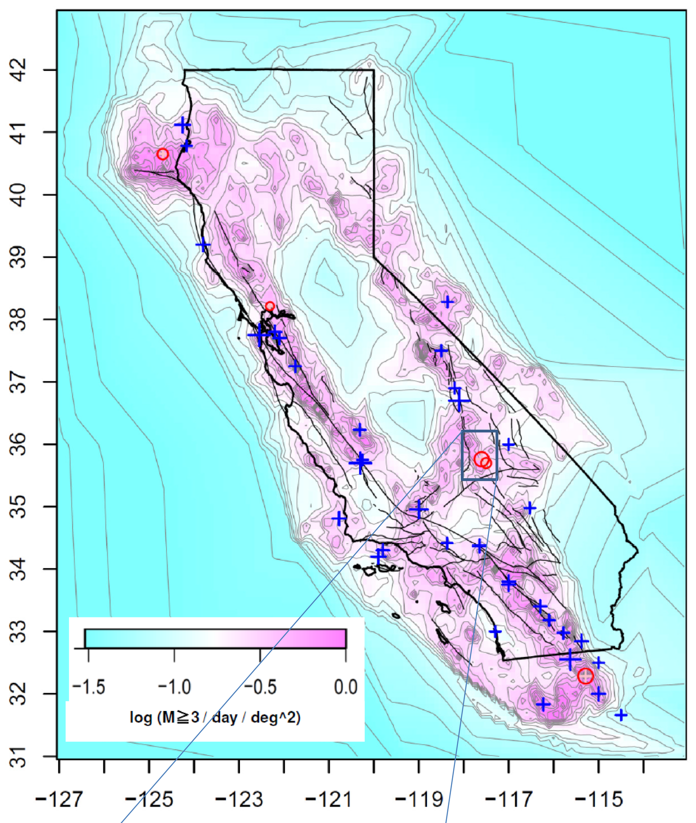

Background seismicity rate in California obtained by the optimal inversion of the 2D piecewise linear function on the Delaunay triangles, estimated from M ≥ 3.0 earthquakes in ANSS catalog for the target interval 2006 – 2011 with the precursory period 1932 – 2005. the contour interval is about three times as large. ○ indicate M ≥ 6.4 earthquakes that occurred 2012 - 2019, and + signs are M ≥ 6.5 earthquakes that occurred 1500 - 2005.

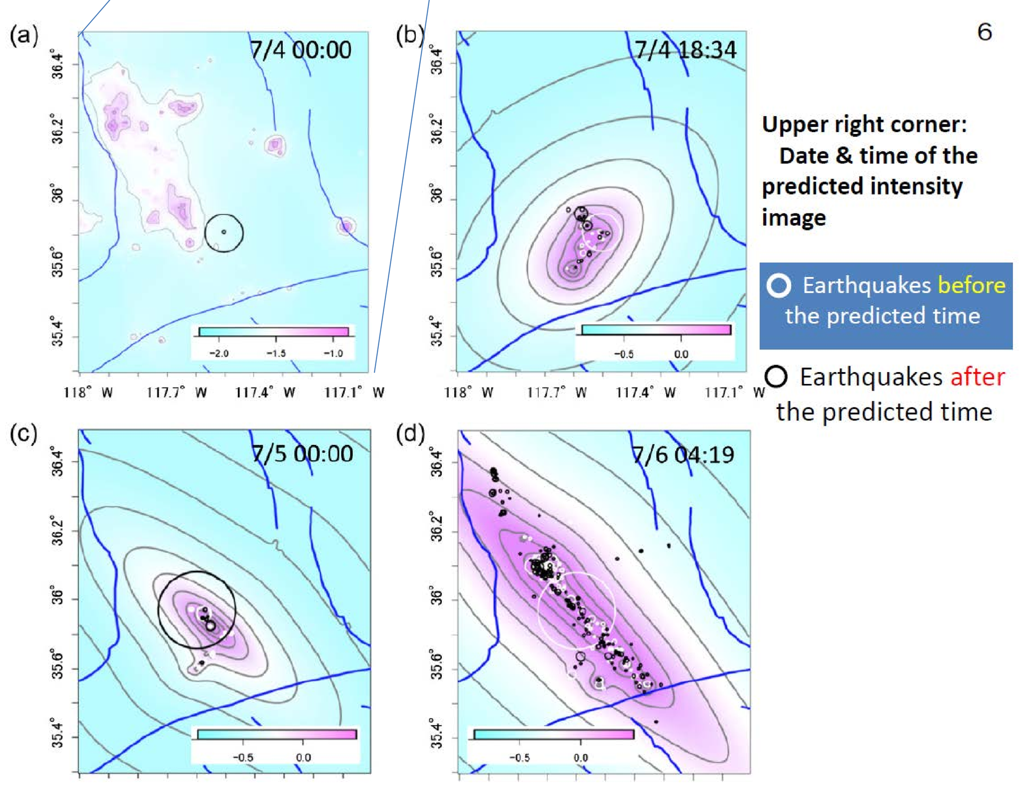

Upper right corner: Date & time of the predicted intensity image

○ Earthquakes before the predicted time

○ Earthquakes after the predicted time

Here is a noteworthy snapshot. Panel (a) shows just before M6.4, (b) shows just after M6.4, (c) shows before and after the largest aftershock M5.4, and (d) shows after M7.1. In all cases, black circle earthquakes occurred as expected.

Foreshock probability forecasts

Our definition of foreshock-type cluster is having a larger earthquake in the future by the difference of 0.5 magnitude unit (5 times of energy) or larger than the currently largest earthquake.

When the Searles Valley earthquake and its aftershocks occur, we calculate their foreshock probabilities.

Single-link-clustering by connecting the space-time distance

$$d_{ST}=\sqrt{\Delta^2_{space}+(c\Delta_{time})^2}\le 0.3^\circ\ (\text{or }30\text{km})$$

The statistics for the California region were taken for the earthquake cluster. The percentage of foreshock type earthquakes ranges from 4% to 10% of them.

The number of clusters and isolated earthquakes of M ≥ 3.5 over the period 1932–2007.

#Earth-quakes in a cluster	#Foreshock type clusters	Foreshock clusters ratio(%)	#Swarm-type clusters	#Aft-shock type clusters	#All types clusters
≥ 1	115	(4.2 ± 0.4)	200	2429	2744
≥ 2	44	(7.8 ± 1.1)	200	322	566
≥ 3	23	(8.3 ± 1.7)	110	144	277
≥ 4	16	(9.6 ± 2.3)	67	84	167
≥ 5	13	(10.8 ± 2.8)	51	56	120
≥ 6	6	(6.7 ± 2.6)	40	44	90
≥ 7	5	(7.6 ± 3.3)	28	33	66
≥ 8	3	(5.9 ± 3.3)	23	25	51
≥ 9	3	(6.8 ± 3.8)	19	22	44
≥ 10	2	(4.9 ± 3.4)	17	22	41

Especially isolated earthquakes make up 80% of the total. When an isolated earthquake or the first earthquake of a cluster occurs, there is a 4.2% chance that it is of the foreshock type, whereas the Ridge crest area is close to 10% as seen below figures.

Probability forecast of the first or isolated event

One-month probability of foreshock-type clusters with different logit models.

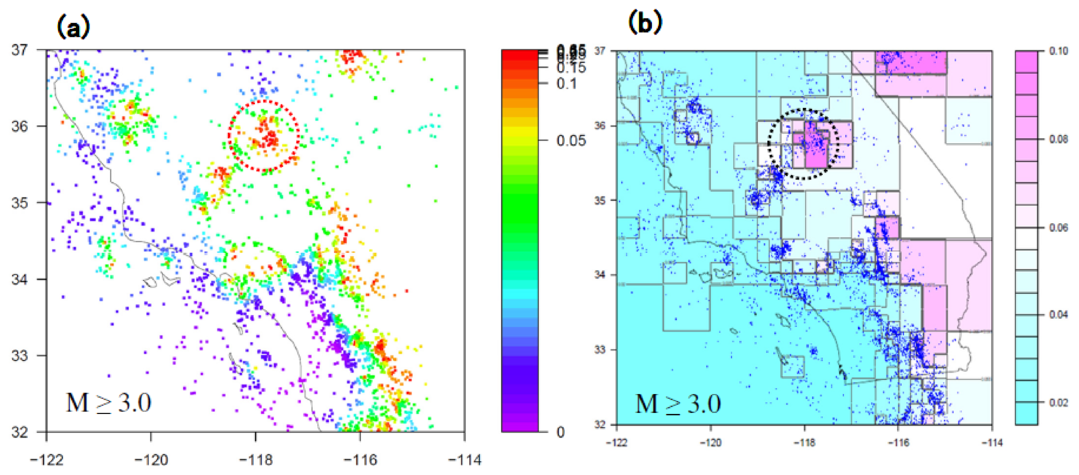

Colored dots in (a) and blue dots in (b) are isolated earthquakes or first earthquakes in the Single Linked clusters. **Color tables** indicate the probability having an earthquake with magnitude M+0.5 or larger in the future, where the first earthquake is magnitude M.

Cross classified table analysis

First event in a cluster or isolated event

Goodness of fit of regional dependency against constant probability (with an average of 4.2%)

TABLE 2
Evaluation of the Regional Forecasts of Earthquake Units

Forecast (%)	0–2.5	2.5–5.0	> 5.0	All
Foreshocks	8	41	66	115
Others	680	1291	658	2629
All	688	1332	724	2744
Ratio (%)	1.2	3.1	9.1	4.2

An evaluation of the regional forecasts of earthquake units, depending on the location of the first earthquake within a cluster or an isolated earthquake. "Ratio (%)" indicates the fraction of true foreshock clusters to forecast foreshock clusters. The significance of this contingency table against the generic forecast of 4.2% is given by ΔAIC = −55.44.

Probability forecast for the plural events

Excluding isolated earthquakes, the average probability of becoming a foreshock type increases to 8%, but the predicted probability ranges from 1% to 30%.

Hit ratio of the forecasts for multiple earthquakes

TABLE 3
Evaluation of Cross-Classified Performance

Forecast (%)	0–4	4–8	8–12	12–16	> 16	All
Foreshocks	1	28	15	4	3	51
Others	131	284	146	22	7	590
All	132	312	161	26	10	641
Ratio (%)	0.8	9.0	9.3	15.4	30.0	8.0

Evaluation of the cross-classified performance, including the forecast of multiple earthquakes. "Ratio (%)" indicates the fraction of actual foreshock clusters. The significance of the contingency table against the generic forecast of 8.0% is ΔAIC = −13.54. The information gain score is 8.3 for the binomial experiments, against a generic forecast of 8.0%.

Early aftershock forecasts

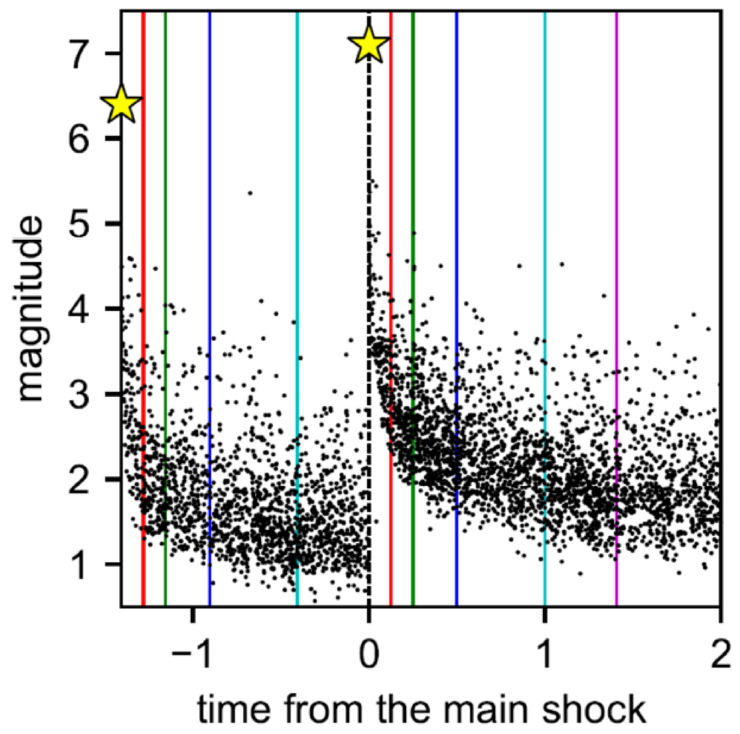

Aftershocks detected as part of the Searles Valley and Ridgecrest earthquake sequence.

Plots of magnitude versus time for the 2019 Ridgecrest aftershock sequences from the early edition of the ANSS ComCat. Two stars represent the Mw 6.4 Searles Valley earthquake and the M7.1 Ridgecrest earthquake, respectively. Vertical lines (colored) are the time of the aftershock forecast over the next 24 hr span; red, green, blue, light blue, and purple lines represent 3, 6, 12, 24, and 33.7 hr, respectively.

Reasenberg-Jones model with detection function

$$\lambda(t,M)=\frac{K\cdot 10^{-bM}}{(t+c)^p}\int_{-\infty}^{M}\frac{1}{\sqrt{2\pi}}e^{-\frac{(z-\mu(t))^2}{2\sigma^2}}dz$$

$$\Lambda(M;S,T)=\int_M^\infty dM\int_S^T\frac{K\cdot 10^{-bM}}{(t+c)^p}dt$$

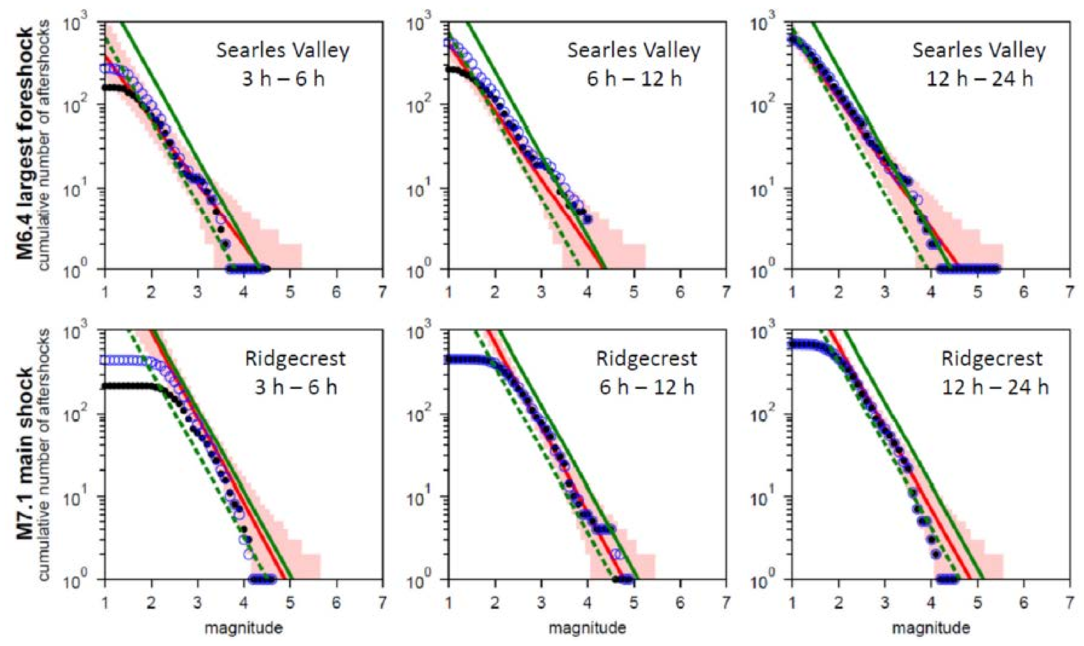

Frequency distribution of aftershocks for these time intervals for the Searles Valley earthquake. **Black disks** are empirical distributions of aftershocks immediately after, and **blue circles** are empirical distributions of aftershocks based on data after 6 months. The **solid red line** shows the predicted distribution of aftershocks by the real-time model, and the **solid** and **dotted green lines** show the predictions made using a general-purpose model for the Coso volcanic region and Southern California region here. For aftershock of Ridgecrest. **In each case, the real-time model is excellent.**

One-day (24 hr) probability forecasts of aftershock that exceed magnitude M_t

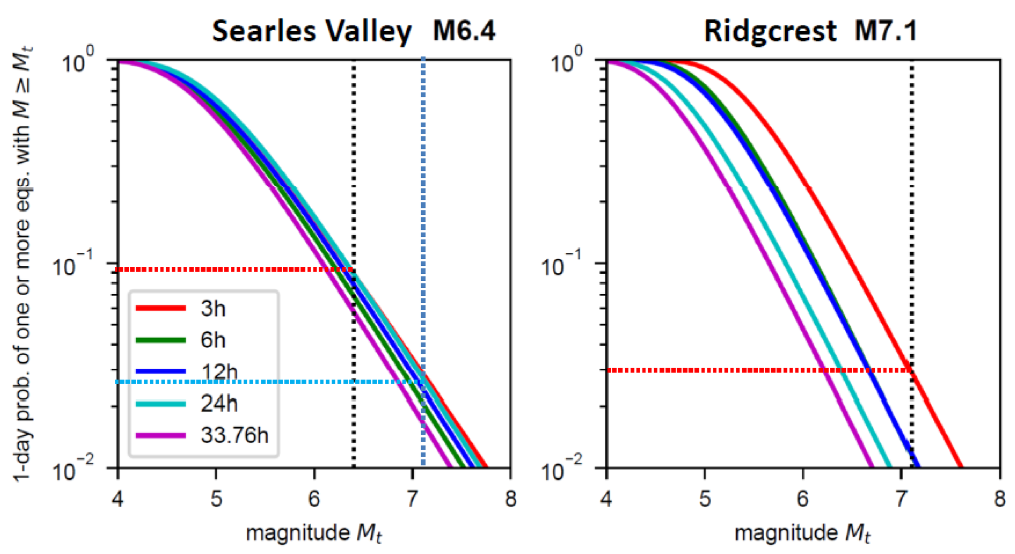

These show aftershock probability during one day (24 hours) span when aftershock exceeding magnitude M_t will occurs. Forecasts are created using aftershock data till the indicated elapsed time after the main shock. In addition, vertical dotted lines and horizontal dotted lines are used to indicate the probability of occurrence of aftershocks larger than the main shock.

Occurrence probability of at least one aftershock of M ≥ 6.0 within the following one day (24 hr).

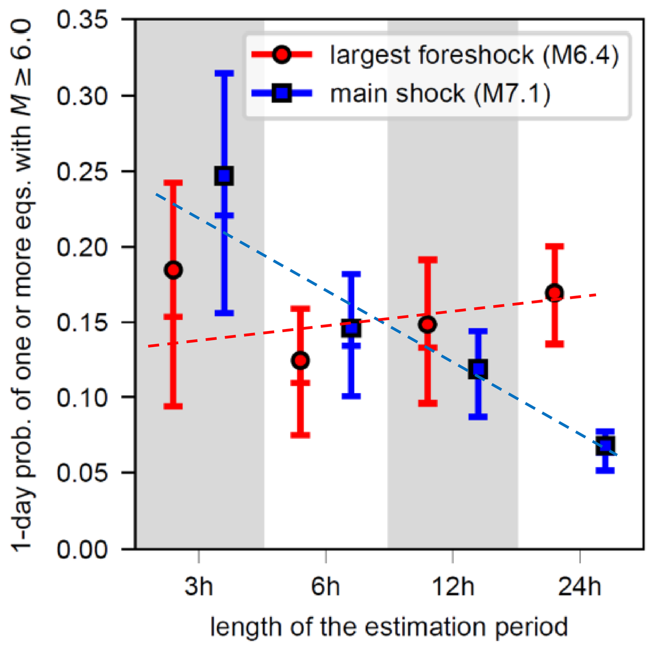

Confidence bars with circle and squares indicate one-day (24 hr) probability forecasts for an **M ≥ 6.0 aftershock** at the indicated time after **Searles Valley** and **Ridgecrest** earthquakes, respectively. The circles and squares are the MLEs, and other markers on the confidence bars represent the 25th, 50th, the average, and 75th percentiles of the forecast probabilities.

Difference of the parameter values between the two aftershock sequences

$$\lambda_\theta(t,M)=\frac{K\cdot 10^{-bM}}{(t+c)^p}\int_{-\infty}^{M}\frac{1}{\sqrt{2\pi}\sigma(t)}e^{-(z-\mu(t))^2/\sigma(t)^2}$$

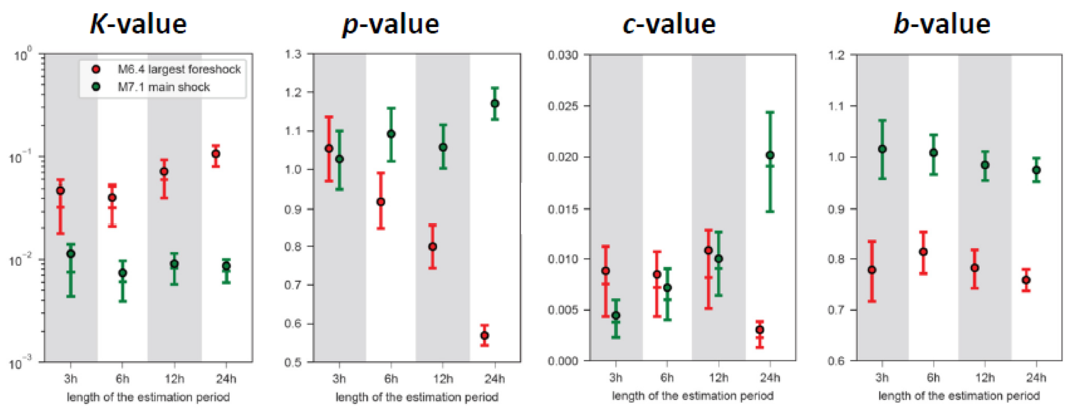

Estimated parameters of the Reasenberg–Jones model at lapsed time from the Mw 6.4 Searles Valley and Mw 7.1 Ridgecrest earthquakes, respectively. The MLEs of (a) K-, (b) p-, (c) c-, and (d) b-values are shown with their 25th, 50th, and 75th percentiles calculated from the respective marginal posterior distributions, for which the scale unit is event/day, no dimension, 1/day, and 1/magnitude, respectively.

Space-Time anomalies in aftershock activity

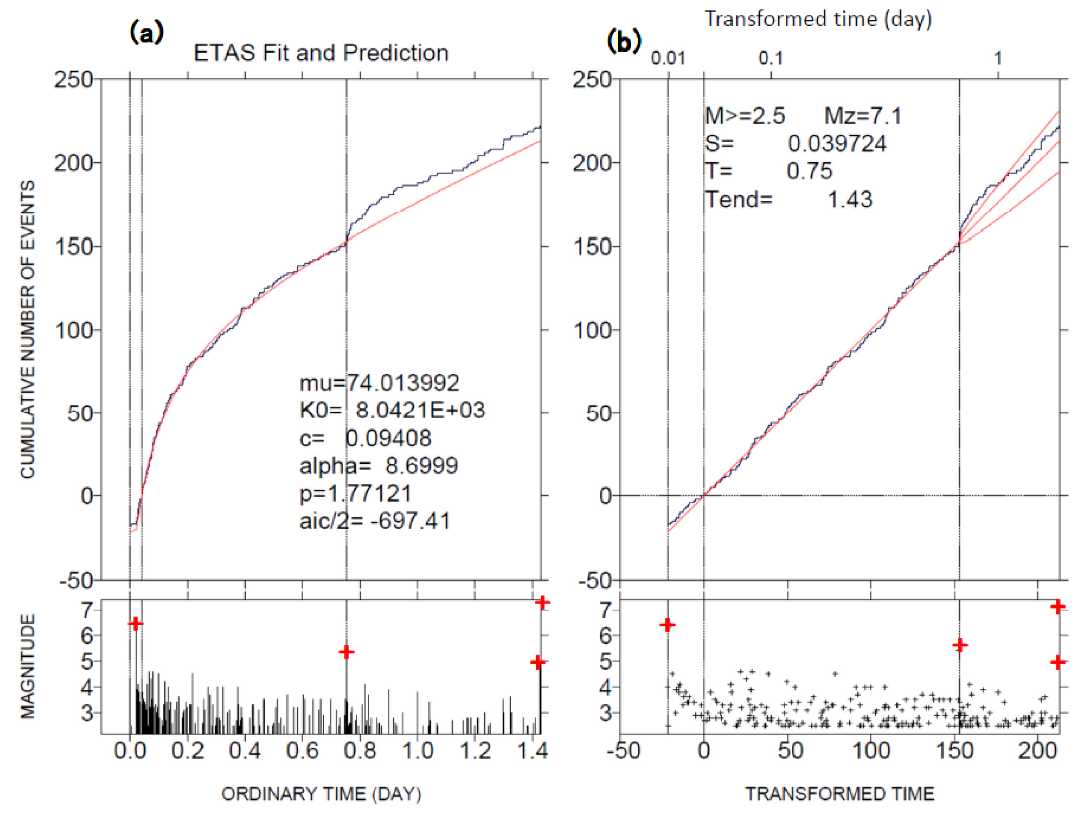

In the Searles Valley aftershock sequence, the ETAS model fits well in the period leading up to the dashed line. This ETAS model has a very large **alpha** value and is equivalent to the Omori-Utsu formula.

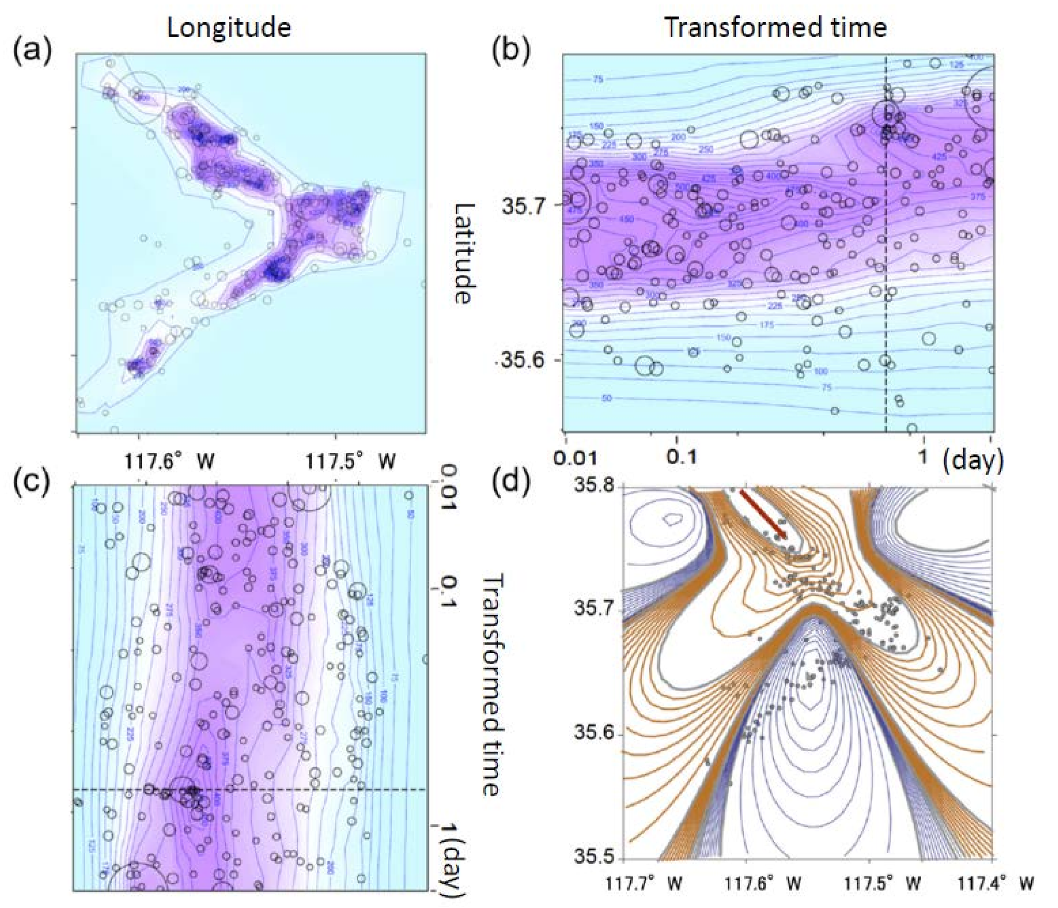

Panels (b,c) are seismic densities in space-time over the transformed time axis. The contour line is in a linear scale of the densities, with purple being the high density. They are migrated from the time around dashed line. To illustrate this, we assume such a slow slip and the incremental Coulomb stresses are migration-supported.

Key points

- The Ridgecrest earthquake sequence was used to study the potential for real-time forecasting and diagnoses.
- We examine practical forecasting using short-term ETAS models combined with longer-term probabilities.
- Operational, real-time, multiple element probability forecasting appears plausible.

References

Ogata, Y. and Omi, T. (2020). Statistical Monitoring and Early Forecasting of the Earthquake Sequence: Case Studies after the 2019 M 6.4 Searles Valley Earthquake, California, Bulletin of the Seismological Society of America, 110 (4), 1781–1798, https://doi.org/10.1785/0120200023

Ogata, Y. (2017a). Forecasting of a Large Earthquake: An outlook of the research, *Seismological Research Letters* **88** (4), 1117–1126, doi:10.1785/0220170006.

Ogata, Y. (2017b). Statistics of Earthquake Activity: Models and Methods for Earthquake Predictability Studies, *Annual Review of Earth and Planetary Sciences* **45**, 497-527, doi:10.1146/annurev-earth-063016-015918